



ERNEST ORLANDO LAWRENCE BERKELEY NATIONAL LABORATORY

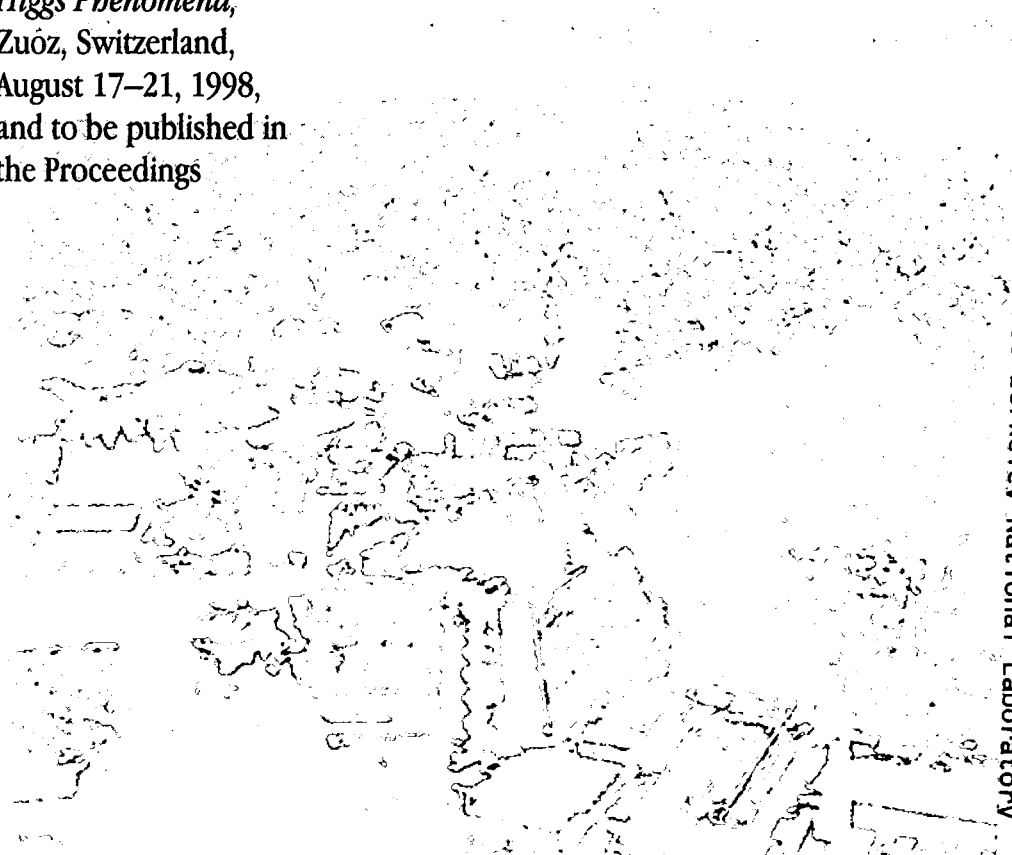
Strong WW Scattering at the End of the 90's: Theory and Experimental Prospects

Michael S. Chanowitz

Physics Division

November 1998

Presented at the
*Zuoz Summer School on
Hidden Symmetries and
Higgs Phenomena,*
Zuöz, Switzerland,
August 17–21, 1998,
and to be published in
the Proceedings



REFERENCE COPY
Does Not
Circulate

Bldg. 50 Library - Ref.
Lawrence Berkeley National Laboratory

Copy 1

LBNL-42570

DISCLAIMER

This document was prepared as an account of work sponsored by the United States Government. While this document is believed to contain correct information, neither the United States Government nor any agency thereof, nor the Regents of the University of California, nor any of their employees, makes any warranty, express or implied, or assumes any legal responsibility for the accuracy, completeness, or usefulness of any information, apparatus, product, or process disclosed, or represents that its use would not infringe privately owned rights. Reference herein to any specific commercial product, process, or service by its trade name, trademark, manufacturer, or otherwise, does not necessarily constitute or imply its endorsement, recommendation, or favoring by the United States Government or any agency thereof, or the Regents of the University of California. The views and opinions of authors expressed herein do not necessarily state or reflect those of the United States Government or any agency thereof or the Regents of the University of California.

Strong WW scattering at the end of the 90's: theory and experimental prospects ¹

Michael S. Chanowitz²

*Theoretical Physics Group
Lawrence Berkeley National Laboratory
University of California
Berkeley, California 94720*

Abstract

The nature of electroweak symmetry breaking can only be established definitively by the direct discovery and detailed study of the symmetry breaking quanta at high energy colliders. At the LHC the ability to observe TeV scale strong WW scattering confers a no-lose capability to establish the mass scale and interaction strength of the symmetry breaking quanta, even if the symmetry breaking quanta resist discovery and whether strong WW scattering is observed or excluded. This lecture discusses the motivation to consider strong WW scattering in light of what we have learned from precision electroweak data during the decade. The theoretical basis for strong WW scattering is explained with an introductory review of the Higgs mechanism from a general perspective that encompasses light, perturbative Higgs bosons or nonperturbative, dynamical symmetry breaking by TeV scale strong interactions. The experimental signals and backgrounds are reviewed and the sensitivity of experiments at the LHC is assessed.

A lecture presented at the Zuoz summer school on Hidden Symmetries and Higgs Phenomena, August 17 -21, 1998, Zuoz, Switzerland, to be published in the proceedings.

¹This work was supported by the Director, Office of Energy Research, Office of High Energy and Nuclear Physics, Division of High Energy Physics of the U.S. Department of Energy under Contract DE-AC03-76SF00098.

²Email: chanowitz@lbl.gov

1. Introduction

Broadly speaking there are two possibilities for electroweak symmetry breaking: weakly coupled Higgs bosons below 1 TeV or a new sector of quanta at the TeV scale that interact strongly with one another *and* with longitudinally polarized W and Z bosons.³ While precision electroweak data accumulated in the 90's favor the first scenario, the conclusion is not definitive. The study of WW scattering at the TeV scale, to begin at the LHC, will provide a no-lose capability to determine the strength and mass scale of the symmetry breaking quanta. As discussed below, it is a fundamental measurement, of interest even if a light Higgs boson candidate were to be discovered before inauguration of the LHC, and it could be crucial if Higgs sector quanta turn out to be more elusive. This lecture is an introduction to the motivation, theory, and techniques for the study of WW scattering at the TeV scale. In particular I will focus on the generic strong WW scattering signal[1] that can be used at the LHC to determine definitively whether the symmetry breaking force is weak or strong. Because we would learn from the presence or absence of strong WW scattering whether the symmetry breaking physics is at or below the TeV scale, ability to measure or exclude the signal confers a “no-lose” capability to determine the mass scale of symmetry breaking.

While the precision electroweak data favors the weak breaking scenario, the strong WW scattering measurement remains an important tool for the study of symmetry breaking:

First, because the precision electroweak data probes the Higgs quanta only indirectly, by means of quantum corrections, it can never definitively determine the nature of the Higgs sector. The relevant quantum corrections are open to contributions from many forms of new physics. Occam's razor favors the simplest interpretation, which assumes that the only new physics contributing significantly to the radiative corrections is the quanta that form the symmetry breaking condensate. In that case the data do favor weak symmetry breaking. But nature may well have dealt us a more complicated hand, with new physics accompanying the symmetry breaking quanta also contributing to the radiative corrections. Then the precision data tells us nothing about the symmetry breaking sector — unless we can “unscramble” the different contributions, which in general we do not know how to do. While my focus is on general aspects and not on specific models, reference [2] lists a few models of strong symmetry breaking that can serve as existence proofs. The nature of the symmetry breaking sector can only be established definitively by its direct discovery and detailed study in experiments at high energy colliders. In the meantime it is sensible to be guided by compelling theories, e.g., SUSY, but not to rely on them exclusively.

Second, even if there were a light Higgs boson it is possible for it to be undetectable at all planned experiments up to and including the LHC. For example, Gunion, Haber, and Moroi[3] have found “blind spots” in the parameter space of the NMSSM (the next-to-minimal model, containing a Higgs singlet field in addition to the fields of the MSSM) for which none of the Higgs scalars could be discovered at LEP or the LHC, even if the LHC were to accumulate the heroic integrated luminosity of 600 fb^{-1} . In that case the “no-lose” capability of the LHC would be crucial to establish whether electroweak symmetry breaking is weak or strong. As discussed in this lecture, with $\simeq 100 - 150 \text{ fb}^{-1}$ the LHC could observe or exclude strong WW scattering.[4, 5, 6] In a blind-spot scenario it could

³In this sense, theories with TeV scale strong dynamics that engenders a light composite Higgs scalar which breaks $SU(2) \times U(1)$ are classified as weakly coupled.

establish the absence of strong WW scattering which would tell us to look harder for light Higgs scalars below 1 TeV, perhaps with an electron collider.[7] Or, if strong WW scattering were observed, it would tell us to look for the Higgs sector quanta above 1 TeV, perhaps with a VLHC.

Third, even if there were a light Higgs boson and even if it were discovered at LEP, Fermilab, or the LHC, it would still be important to measure the WW scattering cross section in the TeV region. If symmetry breaking is due to a light Higgs boson, a central prediction of the Higgs mechanism is that there be no strong WW scattering. As explained in the review of the Higgs mechanism given below, strong WW scattering is the first-cousin to the famous “bad high energy behavior” which it is the principle mission of the Higgs mechanism to remove. For strong symmetry breaking the unitarity of longitudinal WW scattering is saturated, while for weak breaking, longitudinal WW scattering cuts off while it is still weak, well below where unitarity would be saturated. In discussing the experimental signals at the LHC I will consider both the capability to observe strong WW scattering if it is present and to exclude it if it is not.

The central point is easy to grasp: we have already discovered three quanta from the Higgs sector, the longitudinal spin modes of the W^\pm and Z bosons, which in the Higgs mechanism are the transubstantiated ghosts of Higgs sector quanta. By measuring the scattering of the longitudinal modes $W_L W_L \rightarrow W_L W_L$ (where L denotes longitudinal) we are probing the Higgs sector interactions, a statement made precise by the ‘equivalence theorem.’[8, 9] As reviewed below the absence or presence of an enhanced WW signal at the LHC can then determine if the Higgs sector interactions are weak or strong and correspondingly if the Higgs sector quanta lie below or at the TeV scale.

The lecture is organized as follows:

- Section 2 reviews the Higgs mechanism in a general framework that applies whether Higgs bosons exist or not, using symmetry and unitarity to analyze the possible forms electroweak symmetry breaking may take.
- Section 3 is a brief discussion of the implications of the precision electroweak data presented at the recent Vancouver ICHEP meeting.
- Section 4 reviews models used to estimate strong WW scattering cross sections at high energy colliders.
- Section 5 discusses methods of computing WW scattering at colliders, including the ‘classical’ effective W approximation[10] (EWA) and a more complete method, the effective Higgs bosons representation[11] (EHB), which predicts the experimentally important transverse momentum spectrum of the final state jets recoiling against the WW pair that cannot be obtained from the EWA.
- Section 6 considers the question ‘Can LHC lose?’, reviewing the experimental strategies and the capability of LHC experiments to observe or exclude strong WW scattering.
- A brief conclusion is given in section 7.

2. General Framework

We begin with a general description of the Higgs mechanism in Section 2.1 that applies whether Higgs bosons exist or not. Implications for strong WW scattering are reviewed in the subsequent subsections: the Equivalence Theorem in 2.2, the WW low energy theorems in 2.3, and unitarity and the energy scale of strong WW scattering in 2.4.

2.1 The Generic Higgs Mechanism[12]

The basic ingredients of the Higgs mechanism are a gauge sector and a symmetry breaking sector,

$$\mathcal{L} = \mathcal{L}_{\text{gauge}} + \mathcal{L}_{\text{SB}} . \quad (2.1)$$

$\mathcal{L}_{\text{gauge}}$ is an unbroken *locally symmetric = gauge invariant* theory, describing massless gauge bosons that are transversely polarized, just like the photon. For $SU(2)_L \times U(1)_Y$ gauge symmetry the gauge bosons are a triplet $\vec{W} = W_1, W_2, W_3$ corresponding to the generators \vec{T}_L and a singlet gauge boson X corresponding to the hypercharge generator Y . \mathcal{L}_{SB} is the symmetry breaking Lagrangian that describes the dynamics of the symmetry breaking force and the associated quanta. If \mathcal{L}_{SB} did not exist, the unbroken $SU(2)_L$ nonabelian symmetry would give rise to a force that would confine quanta of nonvanishing \vec{T}_L charge, such as left-handed electrons and neutrinos.

In the generic Higgs mechanism \mathcal{L}_{SB} breaks the *local* (or *gauge*) symmetry of $\mathcal{L}_{\text{gauge}}$. To do so \mathcal{L}_{SB} must possess a *global* symmetry G that breaks spontaneously to a subgroup H ,

$$G \rightarrow H. \quad (2.2)$$

In the electroweak theory we do not yet know either of the groups G or H ,

$$G = ? \quad (2.3a)$$

$$H = ? \quad (2.3b)$$

We want to discover what they are and beyond that we want to discover the symmetry breaking sector

$$\mathcal{L}_{\text{SB}} = ? \quad (2.4)$$

including the mass scale of its spectrum

$$M_{\text{SB}} = ? \quad (2.5)$$

and the interaction strength

$$\lambda_{\text{SB}} = ? \quad (2.6)$$

We do already know one fact about G and H : G must be at least as big as $SU(2)_L \times U(1)_Y$ or \mathcal{L}_{SB} would *explicitly* (as opposed to *spontaneously*) break the $SU(2)_L \times U(1)_Y$ gauge symmetry. Similarly H must be at least as big as $U(1)_{EM}$ or the theory after spontaneous breakdown will not accommodate the unbroken gauge symmetry of QED. That is, in order to be consistent with the desired pattern of breaking for the *local* symmetry

$$SU(2)_L \times U(1)_Y \rightarrow U(1)_{EM} \quad (2.7)$$

the spontaneous breaking of the *global* symmetry of \mathcal{L}_{SB}

$$G \rightarrow H \quad (2.8)$$

is constrained by

$$G \supset SU(2)_L \times U(1)_Y \quad (2.9)$$

$$H \supset U(1)_{EM}. \quad (2.10)$$

There are two steps in the Higgs mechanism. The first has nothing to do with gauge symmetry—it is just the spontaneous breaking of a global symmetry as explained by the Goldstone theorem. By *spontaneous* symmetry breaking $G \rightarrow H$ we mean that

$$G = \text{global symmetry of the interactions of } \mathcal{L}_{\text{SB}} \quad (2.11a)$$

while

$$H = \text{global symmetry of the ground-state of } \mathcal{L}_{\text{SB}}. \quad (2.11b)$$

That is, the dynamics of \mathcal{L}_{SB} are such that the state of lowest energy (the *vacuum* in quantum field theory) has a smaller symmetry group than the symmetry of the force laws of the Lagrangian. Goldstone's theorem tells us that for each broken generator of G the spectrum of \mathcal{L}_{SB} contains a massless spin zero particle or Goldstone boson,

$$\begin{aligned} \# \text{ of massless scalars} &= \# \text{ of broken symmetry axes} = \text{dimension } G - \text{dimension } H \\ &= \# \text{ of energetically flat directions in field space.} \end{aligned} \quad (2.12)$$

The last line is the clue to the proof of the theorem: masses arise from terms that are quadratic in the fields,

$$\mathcal{L}_{\text{mass}} = -\frac{1}{2}m^2\phi^2, \quad (2.13)$$

so a field direction that is locally flat in energy (i.e., goes like ϕ^n with $n \geq 3$) corresponds to a massless mode.

The essential features are the symmetries of the Lagrangian (G) and the ground state (H). Elementary scalars are *not* essential: if necessary Nature will make composite massless scalars. She has (almost) already done so on at least one occasion: we believe on the basis of strong theoretical and experimental evidence that QCD with two (almost) massless quarks is an example, with the pion isotriplet the (almost) Goldstone bosons. The initial global (flavor) symmetry of two flavor QCD in the $m_u = m_d = 0$ limit is

$$G = SU(2)_L \times SU(2)_R \quad (2.14)$$

since we could perform separate isospin rotations on the right and left chirality u and d quarks. The ground state has a nonvanishing expectation value for the bilinear operator

$$\langle \bar{u}_L u_R + \bar{d}_L d_R + h.c. \rangle_0 \neq 0 \quad (2.15)$$

where *h.c.* = hermitian conjugate. The condensate (2.15) breaks the global symmetry spontaneously, $G \rightarrow H$, where

$$H = SU(2)_{L+R} \quad (2.16)$$

is the ordinary isospin group of nuclear and hadron physics. That is, (2.15) is not invariant under independent rotations of left and right helicity quarks but only under rotations that act equally on left and right helicities. In this example $\dim G = 6$ and $\dim H = 3$ so we expect $6 - 3 = 3$ Goldstone bosons. In nature we believe they are the pion triplet, π^+, π^-, π^0 , which are much lighter than typical hadrons because the u and d quark masses are so small on the hadronic scale, of order 10 MeV. (I refer to the “current” quark masses, the parameters that appear in the QCD Lagrangian.)

In the first step we considered only the global symmetry breakdown induced by \mathcal{L}_{SB} — Goldstone’s theorem. Now we come to the second step, which involves the interplay of \mathcal{L}_{SB} with $\mathcal{L}_{\text{gauge}}$. The essential point of the Higgs mechanism is that when a spontaneously broken generator of \mathcal{L}_{SB} coincides with a generator of a gauge invariance of $\mathcal{L}_{\text{gauge}}$, the associate Goldstone boson w and massless gauge boson W mix to form a massive gauge boson. The number of degrees of freedom are preserved, since the Goldstone boson disappears from the physical spectrum while the gauge boson acquires a third (longitudinal) polarization state. Like the first step this is a general phenomenon that depends only on the nature of the global and local symmetries, regardless of whether there are elementary scalar particles in the theory.

Suppose the Goldstone boson w couples to one of the gauge currents, with a coupling strength f which has the dimension of a mass,

$$\langle 0 | J_{\text{gauge}}^\mu | w(p) \rangle = \frac{i}{2} f p^\mu \quad (2.17)$$

f is analogous to F_π , the pion decay constant, that specifies the coupling of the pion to the axial isospin current,

$$\langle 0 | J_5^\mu | \pi(p) \rangle = i F_\pi p^\mu \quad (2.18)$$

Equation (2.17) means that the current contains a term linear in w ,

$$J_{\text{gauge}}^\mu(x) = \frac{1}{2} f \partial^\mu w(x) + \dots \quad (2.18)$$

In the Lagrangian J_{gauge}^μ is by definition coupled to the gauge boson W^μ ,

$$\mathcal{L}_{\text{gauge}} = g W_\mu J_{\text{gauge}}^\mu + \dots \quad (2.19)$$

where g is the dimensionless gauge coupling constant. Substituting Eq. (2.17) we find

$$\mathcal{L}_{\text{gauge}} = \frac{1}{2} g f W_\mu (\partial^\mu w) \dots \quad (2.20)$$

which shows that W_μ mixes in the longitudinal (parallel to \vec{p}) direction with the would-be Goldstone boson w .

We can use (2.20) to compute the W mass.[12] In the absence of symmetry breaking the W is massless and transversely polarized. Therefore as in QED we can write its propagator in Landau gauge,

$$D_0^{\mu\nu} = \frac{-i}{k^2} \left(g^{\mu\nu} - \frac{k^\mu k^\nu}{k^2} \right) \quad (2.21)$$

In higher orders the propagator is the sum of the geometric series due to “vacuum polarization”, i.e., all states that mix with the gauge current. The vacuum polarization tensor is defined as

$$\Pi^{\mu\nu}(k) = - \int d^4k e^{-ik \cdot x} \langle T J^\mu(x) J^\nu(0) \rangle_0 = i \frac{g^2 f^2}{4} \left(g^{\mu\nu} - \frac{k^\mu k^\nu}{k^2} \right) + \dots \quad (2.22)$$

In Eq. (2.22) I have indicated explicitly the contribution from the Goldstone boson pole: the factor $1/k^2$ is just the massless propagator and the factor $(gf/2)^2$ can be recognized from Eq. (2.20). The $g^{\mu\nu}$ term is present since gauge invariance requires current conservation, $k_\mu \Pi^{\mu\nu} = 0$. Since it is a constant term with no absorptive part, it does not affect the spectrum of the theory. (In theories with elementary scalars it arises automatically from the contact interaction given by the Feynman rules.)

Finally we compute the W propagator from the geometric series

$$\begin{aligned} D^{\mu\nu} &= (D_0 + D_0 \Pi D_0 + \dots)^{\mu\nu} = -\frac{i}{k^2} \left(g^{\mu\nu} - \frac{k^\mu k^\nu}{k^2} \right) \left(1 + \frac{g^2 f^2}{4k^2} + \dots \right) \\ &= -i \left(g^{\mu\nu} - \frac{k^\mu k^\nu}{k^2} \right) \frac{1}{k^2} \frac{1}{1 - \frac{g^2 f^2}{4k^2}} = -i \frac{g^{\mu\nu} - \frac{k^\mu k^\nu}{k^2}}{k^2 - \frac{g^2 f^2}{4}}. \end{aligned} \quad (2.23)$$

The massless Goldstone boson pole then induces a shift in the pole of the gauge boson propagator(!), to

$$M_W = \frac{1}{2} g f. \quad (2.24)$$

From the measured value of the Fermi constant,

$$G_F = \frac{g^2}{4\sqrt{2}M_W^2} = \frac{1}{\sqrt{2}f^2} \quad (2.25)$$

we learn that

$$f \simeq 250 \text{ GeV}. \quad (2.26)$$

Customarily instead of f we refer to $v \equiv f$, the so-called vacuum expectation value. This custom, which I will also follow (though in general it is not really correct) derives from theories with elementary scalar fields where $v \equiv f$ is both the coupling strength of the Goldstone boson w to J_{gauge} , as in (2.17), and is also the value of the Higgs boson field in the ground state (i.e., the Higgs boson vacuum condensate). However the derivation just reviewed shows that there is no need for a Higgs boson to exist. The condensate that breaks the symmetry may be that of a composite operator, e.g., Eq. (2.15), which in general has no simple relationship to the parameter $f \equiv v$ defined in (2.17). For instance, in QCD there is no trivial relationship between F_π and $\langle \bar{u}u + \bar{d}d \rangle_0$ (although there is a nontrivial relation involving also the quark and pion masses).

2.2 The Equivalence Theorem

The equivalence theorem[8, 9] is very useful for analyzing the implications of the Higgs mechanism for strong WW scattering. In the U (unitary) gauge the Goldstone boson fields

\vec{w} are absent from the Lagrangian. In R (renormalizable) gauges they do appear in \mathcal{L}_{SB} and in the Feynman rules, though gauge invariance ensures that are not in the physical spectrum. Since they engender the longitudinal gauge boson modes, W_L and Z_L , it is plausible that W_L and Z_L interactions reflect the dynamics of \vec{w} . The equivalence theorem is the precise statement of this proposition,

$$\mathcal{M}(W_L(p_1), W_L(p_2), \dots) = \mathcal{M}(w(p_1), w(p_2), \dots)_R + O\left(\frac{M_W}{E_i}\right). \quad (2.27)$$

As indicated the equality holds up to corrections of order M_W/E_i .

We will see that the equivalence theorem is useful in the derivation of the $W_L W_L$ low energy theorems and that it is also a useful source of intuition for the possible dynamics of strong WW scattering. In addition, it greatly simplifies perturbative computations. For instance, the evaluation of heavy Higgs boson production via WW fusion in unitary gauge requires evaluation of many diagrams with “bad” high energy behavior that cancel to give the final result. But to leading order in the strong coupling $\lambda = m_H^2/2v^2$ it suffices using the equivalence theorem to compute just a few simple diagrams. The result embodies the cancellations of many diagrams in unitary gauge and trivially has the correct high energy behavior. It is very accurate for energies above 1 TeV (of order 1 % or better).

A simple example is instructive. Consider the decay of a heavy Higgs boson to a pair of longitudinally polarized gauge bosons $W_L^+ W_L^-$. In unitary gauge the $HW_L^+ W_L^-$ amplitude is

$$\mathcal{M}(H \rightarrow W_L^+ W_L^-) = gM_W \epsilon_L(p_1) \cdot \epsilon_L(p_2). \quad (2.28)$$

For $m_H \gg M_W$ we neglect terms of order M_W/m_H , so that $\epsilon_L^\mu(p_i) \cong p_i/M_W$ and similarly from $m_H^2 = (p_1 + p_2)^2 \cong 2p_1 \cdot p_2$ we find

$$\mathcal{M}(H \rightarrow W_L^+ W_L^-) = g \frac{m_H^2}{2M_W} + O\left(\frac{M_W}{m_H}\right). \quad (2.29)$$

In a renormalizable gauge the corresponding amplitude can be read off (taking care with factors of 2) from the Hww vertex in the Higgs potential, with the result

$$\mathcal{M}(H \rightarrow w^+ w^-) = 2\lambda v. \quad (2.30)$$

Using the relations $M_W = \frac{1}{2}gv$ and $\lambda = m_H^2/2v^2$ we see that Eqs. (2.29) and (2.30) are indeed equal up to $O(M_W/m_H)$ corrections.

The theorem was first proved in tree approximation[8] and used in a variety of calculations. (Lee *et al.*[8] contains a proof to all orders which does not however apply to matrix elements with more than one external W_L .) Proofs to all orders in both \mathcal{L}_{SB} and $\mathcal{L}_{\text{gauge}}$ are given in [9]. The fact that the theorem holds to all orders in the strong interactions of \mathcal{L}_{SB} is crucial for its applicability to strong WW scattering.

2.3 Low Energy Theorems

Using the equivalence theorem and the general properties of the Higgs mechanism described in Section 2.1 we can derive the low energy theorems for $W_L W_L$ scattering that in turn set the scale for the onset of strong WW scattering. The symmetry breaking pattern of \mathcal{L}_{SB} , $G \rightarrow H$, implies low energy theorems for the Goldstone bosons, which imply

$W_L W_L$ low energy theorems by means of the equivalence theorem. In general the low energy theorems are determined by the groups G and H and by two parameters, the vacuum expectation value v and the ρ parameter, $\rho = M_W^2 / (M_Z^2 \cos^2 \theta_W)$. Recall that we assume that there are no light quanta in \mathcal{L}_{SB} other than w and z . If there are other light quanta in \mathcal{L}_{SB} they may or may not modify the low energy theorems.[13]

Low energy theorems for the $2 \rightarrow 2$ scattering of Goldstone bosons were first derived by Weinberg[14] for pion-pion scattering. Identifying the pion isotriplet with the almost-Goldstone bosons of spontaneous flavor symmetry breaking $SU(2)_L \times SU(2)_R \rightarrow SU(2)_{L+R}$ in hadron physics, Weinberg showed for example that

$$\mathcal{M}(\pi^+ \pi^- \rightarrow \pi^0 \pi^0) = \frac{s}{F_\pi^2} \quad (2.31)$$

where $F_\pi = 93$ MeV is the pion decay constant defined in Eq. (2.18). Equation (2.31) neglects $O(m_\pi^2)$ corrections (which are in fact calculable to leading order and were computed by Weinberg) and is valid at low energy, defined as

$$s \ll \text{minimum}\{m_\rho^2, (4\pi F_\pi)^2\}. \quad (2.32)$$

The low energy theorems can be derived by current algebra or effective Lagrangian methods. The proof has two important features:

- it is valid to all orders in the Goldstone boson self-interactions. This is crucial since those interactions may be strong (as they are for the pion example) so that perturbation theory is a non-starter,
- we needn't be able to solve the dynamics or even to know the Lagrangian of the theory. In fact the $\pi\pi$ low energy theorems were derived in 1966 before QCD was discovered. (And we still don't know today how to compute $\pi\pi$ scattering directly in QCD.)

The current algebra/symmetry method was important in the path followed in the 1960's that led in the early 1970's to the discovery that $\mathcal{L}_{\text{HADRON}} = \mathcal{L}_{\text{QCD}}$. It is similarly useful today in our search for \mathcal{L}_{SB} .

If $G = SU(2)_L \times SU(2)_R$ and $H = SU(2)_{L+R}$ as in QCD, then we can immediately conclude, just as in Eq. (2.31) that¹

$$\mathcal{M}(w^+ w^- \rightarrow zz) = \frac{s}{v^2} \quad (2.33)$$

at low energy,

$$s \ll \text{minimum}\{M_{\text{SB}}^2, (4\pi v)^2\}, \quad (2.34)$$

as in eq. (2.32). Here M_{SB} is the typical mass scale of \mathcal{L}_{SB} and $v \simeq \frac{1}{4}$ TeV. More generally, electroweak gauge invariance requires Eqs. (2.9) and (2.10) from which we can deduce the more general result[13]

$$\mathcal{M}(w^+ w^- \rightarrow zz) = \frac{1}{\rho} \frac{s}{v^2}. \quad (2.35)$$

Equation (2.35) is arguably more soundly based than (2.31) was in 1966, since (2.35) is a general consequence of gauge invariance and the Higgs mechanism while (2.31) was based on inspired guesswork as to the symmetries underlying hadron physics. The low energy theorems are proved by three different methods[13]: perturbatively, by a current algebra derivation similar to Weinberg's, and by the chiral Lagrangian method.

We can next use the equivalence theorem, Eq. (2.27), to turn Eq. (2.35) into a physical statement about longitudinal gauge boson scattering. In particular we have

$$\mathcal{M}(W_L^+ W_L^- \rightarrow Z_L Z_L) = \frac{1}{\rho} \frac{s}{v^2} \quad (2.36)$$

for an energy domain circumscribed by Eqs. (2.34) and (2.27) as

$$M_W^2 \ll s \ll \text{minimum}\{M_{\text{SB}}^2, (4\pi v)^2\}. \quad (2.37)$$

The window (2.37) may or may not exist in nature, depending on whether $M_{\text{SB}} \gg M_W$.

In addition to Eq. (2.36) there are two other independent amplitudes which may be chosen to be $W^+ W^-$ and ZZ elastic scattering. Their low energy theorems are:

$$\mathcal{M}(W_L^+ W_L^- \rightarrow W_L^+ W_L^-) = - \left(4 - \frac{3}{\rho}\right) \frac{u}{v^2}, \quad (2.38)$$

$$\mathcal{M}(Z_L Z_L \rightarrow Z_L Z_L) = 0. \quad (2.39)$$

There are in addition four others that can be obtained by crossing symmetry:

$$\mathcal{M}(W_L^\pm Z_L \rightarrow W_L^\pm Z_L) = \frac{1}{\rho} \frac{t}{v^2}, \quad (2.40)$$

$$\mathcal{M}(W_L^+ W_L^+ \rightarrow W_L^+ W_L^+) = \mathcal{M}(W_L^- W_L^- \rightarrow W_L^- W_L^-) = - \left(4 - \frac{3}{\rho}\right) \frac{s}{v^2}. \quad (2.41)$$

2.4 Unitarity and the Scale of Strong WW Scattering

The threshold energy dependence predicted by the low energy theorems would eventually violate unitarity unless damped. In fact, the low energy theorems are identical with the famous "bad" high energy behavior that the Higgs mechanism was invented to cure — this emerges most clearly in the perturbative derivation.³ Within the Higgs mechanism it is the task of \mathcal{L}_{SB} to cut off the growing amplitudes Eqs. (2.36-2.41). Unitarity implies a rigorous upper bound on the energy at which this must occur. The use of unitarity here is identical to that of Lee and Yang[15] and of Ioffe, Okun, and Rudik[16] who used the growing behavior of fermion-fermion scattering in Fermi's four-fermion weak interaction Lagrangian (also proportional to $G_{Fs} \propto s/v^2$!) to bound the scale at which Fermi's theory must break down — essentially a bound on the mass of the W boson. In fact that bound is precisely half the value of the bound given below for the scale of the symmetry breaking physics.

In particular we use partial wave unitarity. The partial wave amplitudes for the Goldstone scalars (or for the zero helicity, longitudinal gauge bosons) are

$$a_J(s) = \frac{1}{32\pi} \int d(\cos \theta) P_J(\cos \theta) \mathcal{M}(s, \theta) \quad (2.42)$$

where θ is the center of mass scattering angle. Partial wave unitarity then requires

$$|a_J(s)| \leq 1. \quad (2.43)$$

Putting $\rho = 1$ we then find

$$|a_0(W_L^+ W_L^- \rightarrow Z_L Z_L)| = \frac{s}{16\pi v^2} \leq 1 \quad (2.44)$$

so that the interactions of \mathcal{L}_{SB} must intervene to damp the absolute value of the amplitude at a scale Λ_{SB} bounded by

$$\Lambda_{\text{SB}} \leq 4\sqrt{\pi}v \simeq 1.75 \text{ TeV}. \quad (2.45)$$

At the cutoff, $s \cong O(\Lambda_{\text{SB}}^2)$, the $J = 0$ wave is

$$|a_0(\Lambda_{\text{SB}})| \cong \frac{\Lambda_{\text{SB}}^2}{16\pi v^2} \quad (2.46)$$

which relates the strength of the interaction and the energy scale of the new physics. If $\Lambda_{\text{SB}} \lesssim \frac{1}{2} \text{ TeV}$ then $a_0(\Lambda_{\text{SB}}) \lesssim 1/4\pi$, well below the unitarity limit. Then \mathcal{L}_{SB} has a weak coupling and can be analyzed perturbatively. For $\Lambda_{\text{SB}} \gtrsim 1 \text{ TeV}$, we have $|a_0(\Lambda_{\text{SB}})| \gtrsim 1/3$, which begins to approach saturation. Then \mathcal{L}_{SB} is a strong interaction theory requiring nonperturbative methods of analysis.

The cutoff is accomplished by exchange of quanta in the Higgs boson channel (i.e., $J = Q_{\text{EM}} = I_{L+R} = 0$ where I_{L+R} is the ‘custodial’ isospin, the diagonal subgroup of the global $SU_{2L} \times SU_{2R}$ discussed in section 2.1.), so we can identify the cutoff Λ_{SB} with the typical mass scale M_{SB} of the quanta of \mathcal{L}_{SB} ,

$$\Lambda_{\text{SB}} \cong M_{\text{SB}}. \quad (2.47)$$

We can illustrate this with two significant examples. The first is the Weinberg–Salam model, in which s -channel Higgs exchange provides the cutoff. Assume that $m_H \gg M_W$ but that m_H is small enough that perturbation theory is not too bad — say $m_H \simeq 700 \text{ GeV}$ so that $\lambda/4\pi^2 = m_H^2/8\pi v^2 \simeq 1/10$. To leading order the $J = 0$ partial wave is

$$a_0(s) = \frac{s}{16\pi v^2} - \frac{s}{16\pi v^2} \frac{s}{s - m_H^2} \quad (2.48)$$

where the first term arises from $\mathcal{L}_{\text{gauge}}$ and the second from the s -channel Higgs boson exchange due to \mathcal{L}_{SB} , now assumed to be the Weinberg-Salam Higgs sector. For $s \ll m_H^2$ the first term dominates, giving the low energy theorem, Eq. (2.44), as it must. But for $s \gg m_H^2$ the two terms combine to give

$$a_0 \Big|_{s \gg m_H^2} = \frac{m_H^2}{16\pi v^2}. \quad (2.49)$$

Comparing Eq. (2.49) with (2.46) we see that (2.47) is indeed verified, i.e., $\Lambda_{\text{SB}} \cong m_H$.

Consider next a strongly-coupled example. In this case we expect to approximately saturate the unitarity bound,

$$\Lambda_{\text{SB}} \cong 4\sqrt{\pi}v \cong O(2) \text{ TeV}. \quad (2.50)$$

We cannot actually compute M_{SB} in this case but we can relate the problem to one that has been studied experimentally. In hadron physics the analogous saturation scale from the $\pi\pi$ low energy theorems is

$$\Lambda_{\text{Hadron}} \cong 4\sqrt{\pi}f_{\pi} \cong 650\text{MeV} \quad (2.51)$$

which indeed coincides with the mass scale of the lightest (non-Goldstone boson) hadrons, e.g., $m_{\rho} = 770$ MeV. The coincidence is not surprising: we expect resonances to form when scattering amplitudes become strong, as they do at the energy scale of the unitarity bound.

The general lesson can be extracted from the Higgs boson example: the cutoff occurs at a scale $s \simeq M_{\text{SB}}^2$ characteristic of \mathcal{L}_{SB} , and at energies $\sqrt{s} \geq M_{\text{SB}}$ the magnitude of the amplitude is of order

$$|a_0(s)| \cong O\left(\frac{M_{\text{SB}}^2}{(1.8\text{TeV})^2}\right). \quad (2.52)$$

More precisely, M_{SB} is the mass scale of the quanta that make the condensate that generates M_W and M_Z .

For $M_{\text{SB}} \ll 1.8$ TeV, the Lagrangian \mathcal{L}_{SB} is weak, WW scattering is never strong, and the amplitudes are cut off by the exchange of narrow $J = 0$ bosons, i.e., Higgs bosons. In that case M_{SB} is an appropriately weighted (by vev) average of the Higgs boson masses,

$$M_{\text{SB}} = \sqrt{\langle m_H^2 \rangle}. \quad (2.53)$$

If $M_{\text{SB}} \geq 1$ TeV then \mathcal{L}_{SB} is strong and Eq. (2.52) shows that there will be strong WW scattering above 1 TeV. We do not then necessarily expect a Higgs boson but do expect a complex strongly interacting spectrum. We expect resonances to appear at the mass scale M_{SB} at which the partial wave amplitudes become strong, $|a_J(M_{\text{SB}}^2)| \sim O(1)$, which implies $M_{\text{SB}} \sim 1 - 3$ TeV. As discussed below, strong two body vector resonances up to $\simeq 2$ TeV would be observable at the LHC, while if the resonances are even heavier we could still probe \mathcal{L}_{SB} by means of nonresonant strong WW scattering.

3. Electroweak radiative corrections and strong WW scattering

In this section I want to briefly discuss the implications of the precision electroweak data. I will discuss the constraints the electroweak data place on the symmetry breaking sector and give an estimate of the contribution to Z -pole radiative corrections from strong WW scattering. The estimate follows by formulating the K-matrix strong scattering model as an effective Higgs boson theory.[11]. The result agrees with an estimate by Gaillard using the nonlinear sigma model.[17] The effective Higgs formulation is described in more detail in section 5, where it's advantages for the calculation of WW cross sections at high energy colliders are discussed.

For several years standard model fits of the precision electroweak data have favored a rather light mass for the Higgs boson, of the order of 100 - 150 GeV and have strongly excluded the TeV scale. Until this summer the strength of that conclusion has been open to question. Two years ago the R_b anomaly distorted the global fits by favoring a low value for the top quark mass which, because of the $m_t - m_H$ correlation in the radiative corrections, drove the Higgs boson mass to low values. At the time Dittmaier, Schildknecht, and Weiglein[18] observed that excluding the R_b measurement and using the directly measured Fermilab value for m_t resulted in fits allowing m_H to reach the TeV scale.

The quantities in the fit that most directly determine m_H are the Z boson decay asymmetries. The left-right polarization asymmetry, A_{LR} , is the most precise and therefore the most important in the fit. Dittmaier et al.[18] and Gurtu[19] both observed that in the 1996 data the A_{LR} measurement by itself implied a value for m_H that conflicted with the lower limit (then $m_H > 65$ GeV) from direct searches at LEP. Dittmaier et al. found that without A_{LR} and R_b the fitted value of m_H increased further, with 900 GeV allowed at the 1σ CL. Gurtu suggested reconciling the conflict by inflating the errors on all the asymmetry measurements and found that the TeV scale was allowed at the 2σ CL.

In the Summer of 1997 the R_b anomaly had disappeared, but the value of m_H did not change much in the global fit, largely due to the increased precision of A_{LR} . With improved calculations of the radiative corrections[20] A_{LR} by itself then implied a 95% upper limit on m_H at the very same value (77 GeV) that the direct searches implied a 95% lower limit,[21] raising the possibility that the fit was skewed to low m_H . I constructed a fitting algorithm, best formulated in the second of references [21], to incorporate the information from the search limits. The algorithm scales the uncertainties of the asymmetry measurements in conflict with the search limits by a factor reflecting the aggregate confidence level for consistency between the complete set of asymmetry measurements and the search limits. The method is motivated by the S^* scale factor the PDG[22] has long used to fit discrepant data, based on their observation that discrepancies occur more often than chance expectation and are often with hindsight found to result from underestimated systematic errors. Applied to the Summer '97 and Spring '98 data I fits using the algorithm allowed (at 95% CL) values of m_H approaching the TeV scale, contrary to the conventional global fits. As you can imagine the question of how to carry out the fits in the face of the discrepancies with the search limits has been controversial, causing polite disagreement and some bar room brawls.

When the method is applied to the Summer '98 data presented at Vancouver[23] the results agree with the conventional fits. From Summer '97 to Summer '98 A_{LR} and A_{FB}^T increased by 1σ and 0.5σ respectively, with half of the shift in A_{LR} occurring in the Spring '98 data. As of Summer '98 the measurements still conflict with the search limit, each implying $m_H < 90$ GeV at 88% CL while the search experiments have $m_H > 90$ GeV at 95% CL. But the aggregate CL for consistency between the nine asymmetry measurements and the search limits increased from $\simeq 0.07$ in Summer '97 to $\simeq 0.12$ in Spring '98 to $\simeq 0.3$ in Summer '98. The latter CL is not small and the algorithm gives essentially no correction to the conventional fit. The algorithm is then useful not only for alerting us to possible problems but for clarifying when apparent discrepancies are not in fact significant.

The contribution of strong WW scattering to the radiative corrections is just one of the ways that a strong symmetry breaking sector could affect the electroweak radiative corrections. It is interesting to estimate the size of its contribution, though it is important to keep in mind that there may be other contributions, possibly with different signs, and to take care to avoid double counting. Naively one would expect strong WW scattering to contribute like a TeV scale Higgs boson. This expectation is confirmed by two different estimates, both heuristic, which find that the contribution is like that of a Higgs boson with mass

$$m_H = \sqrt{\frac{8\sqrt{2}\pi}{G_F}} = 4\sqrt{\pi}v \simeq 1.75\text{TeV} \quad (3.1)$$

which is precisely the unitarity cutoff scale defined in eq. 2.45. This does not mean that such a Higgs boson would exist but only that the contribution to the radiative corrections is like what would naively be expected if it made sense to consider a Higgs boson of that mass.

This estimate was obtained by Gaillard[17] from the nonlinear sigma model with a cutoff that is naturally identified with the cutoff in eq. 2.45. I will sketch a heuristic derivation using a gauge invariant formulation of strong WW scattering, discussed in the next section, in which strong WW scattering models are given an effective Higgs boson representation. Though models of strong WW scattering are formulated in renormalizable gauges using the Goldstone boson ww degrees of freedom, it is possible (and useful for the study of collider signals) to express the models in other gauges including unitary gauge.[11]

We consider the K-matrix model, a model of strong WW scattering described in section 4, that smoothly extrapolates the leading ww partial wave amplitudes from the threshold region, where they are given by the low energy theorems, eqs. 2.36 - 2.39, to higher energy in a way that exactly satisfies elastic unitarity. For the $I = J = 0$ partial wave the K-matrix amplitude is

$$a_{00}^K = \frac{x_{00}}{1 - ix_{00}} \quad (3.2)$$

where x_{00} is the low energy theorem amplitude,

$$x_{00} = \frac{s}{16\pi v^2}. \quad (3.3)$$

As described in section 5, the corresponding effective Higgs propagator is

$$P^K(s) = \frac{i}{s + 16\pi i v^2}. \quad (3.4)$$

Interpreted heuristically as a Breit-Wigner ‘‘resonance’’ the pole in eq. 3.4 corresponds to a ‘resonance’ whose width is twice its mass, $\Gamma_H = 2m_H$. Used naively to evaluate the one loop radiative corrections, the ‘Higgs’ propagator in equation 3.4 induces radiative corrections of the standard model form with m_H given by eq. 3.1, except for a small additional term from the log of the imaginary phase of the pole position.

To summarize, it appears even to a skeptic that the precision electroweak data now exclude strong symmetry breaking dynamics unless associated new physics contributes radiative corrections that offset the contribution from strong WW scattering. It is more natural than not that there be additional contributions, and models [2] have been constructed which are consistent with the precision data. We can regard them as existence proofs that strong WW dynamics may be consistent with the existing data. The definitive tests require TeV scale high energy colliders, starting with the LHC.

4. Models of strong WW scattering

At the LHC the initial goal of experimental study of WW scattering at the TeV scale is to determine whether or not strong scattering occurs. If it does, detailed studies will require even more powerful colliders.[24] In the spirit of the initial, exploratory studies the models of strong WW scattering discussed here are not intended as real dynamical theories but are meant only to provide estimates of the order of magnitude of the expected cross sections in a way that does not conflict with general principles such as unitarity.

To get in the spirit of the exercise, the crudest example is the linear model[1], that uses the threshold amplitudes, eqs. (2.36 - 2.41), which are purely real, as a model of the absolute value of the partial wave amplitudes below the unitarity limit and sets the absolute value of the partial wave amplitudes equal to one at higher energies. For instance, for the $I, J = 0, 0$ partial wave the model is

$$|a_{00}| = \frac{s}{16\pi v^2} \theta(16\pi v^2 - s) + \theta(s - 16\pi v^2). \quad (4.1)$$

The discontinuity in the derivative is unphysical but the model is nonetheless a potentially useful guide to the *magnitude* of certain partial waves. It gives a surprisingly good description of the pion scattering data in the $I = J = 0$ channel — see figure 3.2 of ref.[25]

K-matrix unitarization is perhaps a step up from the linear model,[26] constructed to explicitly satisfy elastic unitarity. Partial wave unitarity is equivalent to the statement that

$$\text{Im}(a_J^{-1}) = -1 \quad (4.2)$$

so that a unitary a_J is completely specified by specifying its real part. For instance, for the isoscalar channel we choose

$$\text{Re}(a_{00}^{-1}) = \frac{16\pi v^2}{s}, \quad (4.3)$$

in order to satisfy the low energy theorem. The K-matrix amplitude is then

$$a_{00} = \frac{s}{16\pi v^2} \left(1 - i \frac{s}{16\pi v^2} \right)^{-1}. \quad (4.4)$$

For the like-charge $I, J = 2, 0$ channel the analogous model amplitudes are

$$|a_{20}| = \frac{s}{32\pi v^2} \theta(32\pi v^2 - s) + \theta(s - 32\pi v^2) \quad (4.5)$$

and

$$a_{20} = -\frac{s}{32\pi v^2} \left(1 + i \frac{s}{32\pi v^2} \right)^{-1}. \quad (4.6)$$

Since we are modeling Goldstone boson scattering we can get some guidance from the $\pi\pi$ scattering data. For the $I = 1$ and $I = 2$ amplitudes the data illustrates the complementarity of the resonant and nonresonant channels. In the $I = 1$ channel the linear model drastically underestimates the magnitude of the amplitude because it omits the large enhancing effect of the ρ resonance. In the $I = 2$ channel it tracks the data fairly well until about $\simeq 600$ MeV (analogous to $\simeq 1.6$ TeV in $W_L W_L$ scattering) where it begins to overestimate the data for the magnitude of the amplitude. This is *also* a consequence of the ρ resonance, which together with the constraints of chiral symmetry, *suppresses* the $I = 2$ amplitude. If $\rho(770)$ were heavier and/or less strongly coupled to $\pi\pi$, the linear model would be a better fit to the data in both the isovector and isotensor channels. The a_{11} amplitude would then be smaller while $|a_{20}|$ would be bigger!

The chiral lagrangian with the ρ meson incorporated in a chiral invariant fashion is a useful tool to illustrate complementarity of resonant and nonresonant scattering signals. Weinberg[27] showed that chiral invariance requires the conventional $\rho\pi\pi$ interaction,

$$\frac{1}{2} f_{\rho\pi\pi} \epsilon_{ijk} \rho_i^\mu \pi_j^\dagger \partial_\mu \pi_k, \quad (4.7)$$

Figure 1a

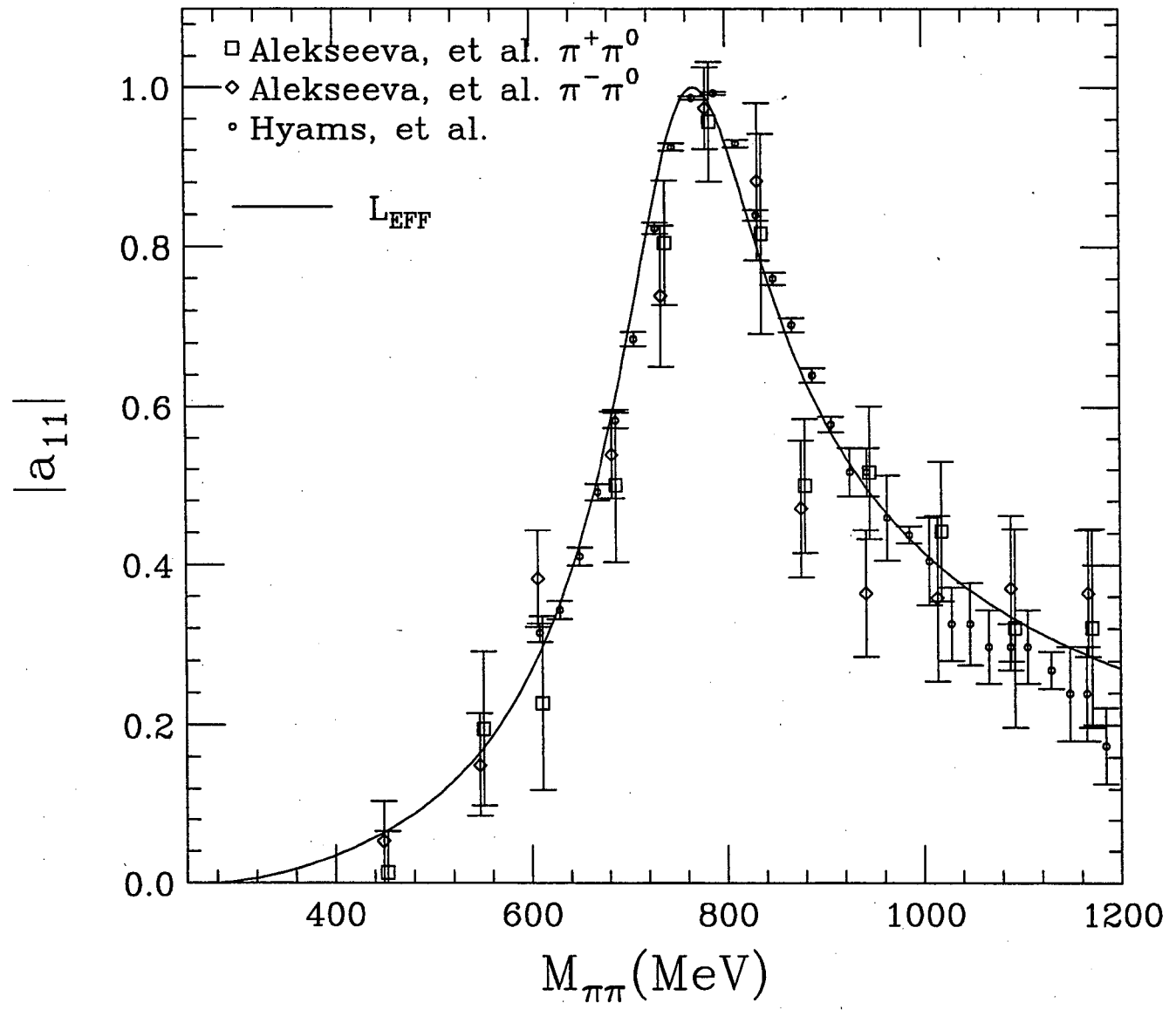
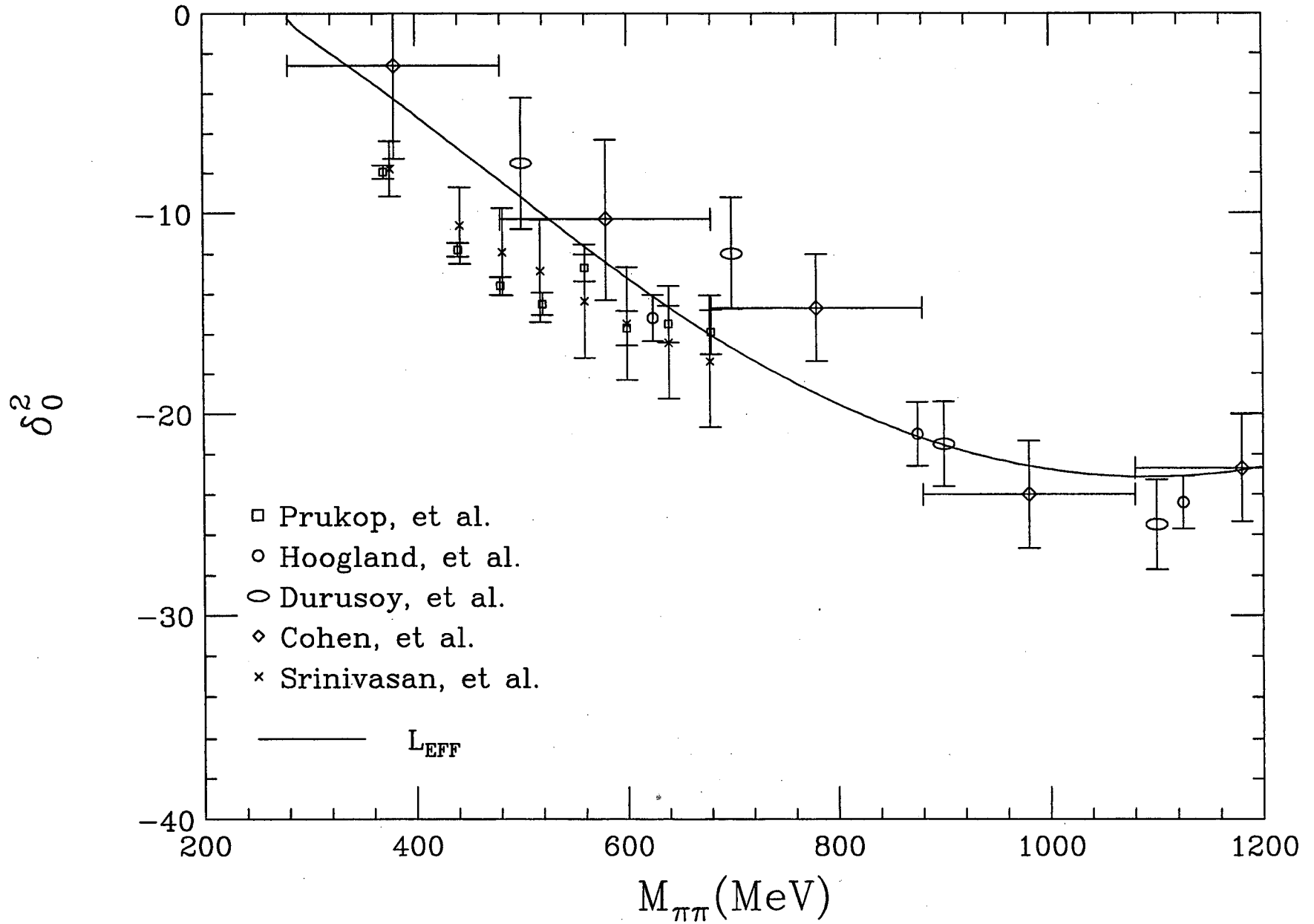


Figure 1b



to be accompanied by a four pion contact interaction that induces a term linear in s in the $\pi\pi$ scattering amplitude. This term cancels the linear terms induced by ρ exchanges, so that the low energy theorems are guaranteed.

This chiral lagrangian gives a remarkably good fit (with no free parameters) to the $\pi\pi$ data for the a_{11} and a_{20} partial waves, for energy as large as 1.2 GeV, shown in figure 1.[4] The quality of the fit at 1.2 GeV must be fortuitous since the linear terms contributed by the chiral lagrangian are irrelevant at that scale. Nevertheless the chiral lagrangian gives a good parameterization of the QCD data, which we can use to explore the consequences of varying the ρ mass and width. For massless Goldstone bosons w_i the ρ width is given by

$$\Gamma_\rho = \frac{f_{\rho ww}^2}{48\pi} m_\rho. \quad (4.8)$$

The Lagrangian is completely specified by the Goldstone boson – gauge current coupling v , and the ρ mass and width. (With an additional direct ρ coupling to fermions, it is also the basis of the BESS model.[28])

To represent possible WW vector resonances we consider two examples of “ ρ ” mesons from minimal, one doublet technicolor, $N_{TC} = 2$ and 4. With the conventional large N_{TC} scaling the mass and width are given in terms of the parameters of the $\rho(770)$ by

$$m_{\rho_{TC}} = \sqrt{\frac{3}{N_{TC}}} \frac{v}{F_\pi} m_\rho \quad (4.9)$$

and

$$\Gamma_{\rho_{TC}} = \frac{3}{N_{TC}} \frac{m_{\rho_{TC}}}{m_\rho} \frac{1}{\beta_\pi^3} \Gamma_\rho. \quad (4.10)$$

where β_π is the pion velocity in the $\rho(770)$ decay. For $N_{TC} = 4$ the mass and width are 1.78 and 0.326 TeV. For $N_{TC} = 2$ they are 2.52 and 0.92 TeV. For larger values of N_{TC} and with the addition of more techniquark doublets the ρ_{TC} becomes lighter and more easily observable. To represent the possibility that the resonances of \mathcal{L}_{SB} may be heavier than the naively anticipated 1 - 3 TeV region I also consider a 4 TeV “ ρ ” meson with a width of 0.98 TeV determined from the $f_{\rho\pi\pi}$ coupling of the $\rho(770)$.

The amplitudes are unitarized by the K-matrix method. The width is omitted in the real part of the s-channel pole contribution and the imaginary part (i.e., the width) is determined from the K-matrix prescription. This is equivalent to the conventional broad resonance Breit-Wigner parameterization with the fixed imaginary part of the denominator, $m\Gamma$, replaced by $\sqrt{s}\Gamma(\sqrt{s})$.

The complementarity of the a_{11} and a_{20} channels is evident in figure 2.[4] As m_ρ increases, the ρ Lagrangian amplitudes approach the nonresonant K-matrix model amplitude for $|a_{11}|$ from above and $|a_{20}|$ from below, since chiral invariant ρ exchange enhances the former and suppresses the latter. At the LHC the 4 TeV “ ρ ” signal is indistinguishable from the signal of the nonresonant K-matrix model. The fact that the “ ρ ” resonance amplitude approaches the nonresonant K-matrix amplitude for large “ ρ ” mass is a very general feature, independent of the specific properties of vector meson exchange. It explains the sense in which smooth unitarization models, such as the linear and K-matrix models, are conservative: they

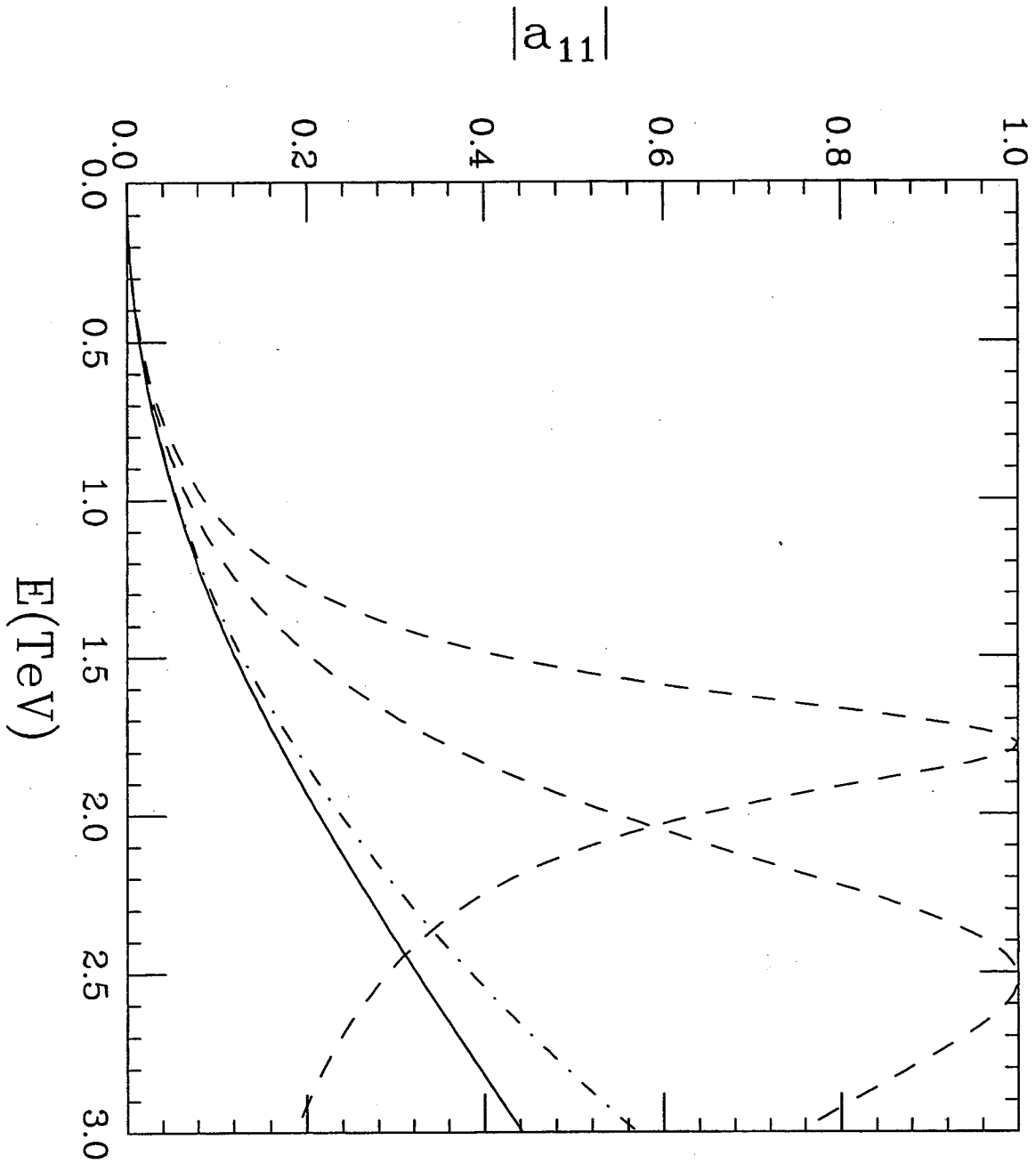
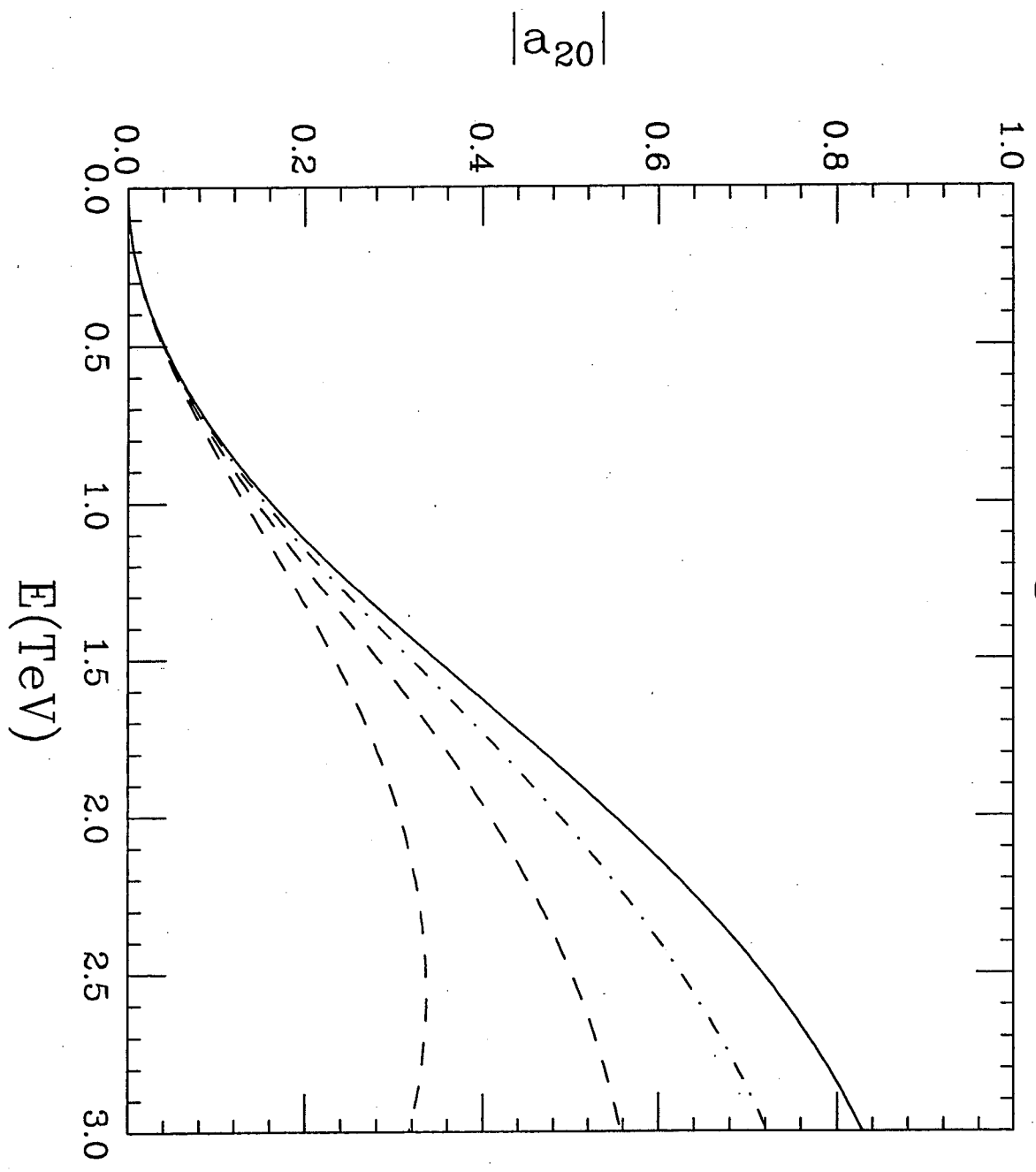


Figure 2a

Figure 2b



represent the “fail-safe” nonresonant scattering signals that are anticipated if the resonances are unexpectedly heavy. This is the most general meaning of complementarity. A more specific meaning, special to vector meson exchange as constrained by chiral symmetry, is the inverse relationship of the $I = 1$ and $I = 2$ channels.

5. Strong WW scattering cross sections at high energy colliders: EWA and EHB

This section is concerned with tools to translate models of WW scattering into collider cross sections. The now traditional method is the effective W approximation[10] (EWA), which is computationally convenient and sufficiently accurate within the experimentally relevant domain of applicability. However, because it is a small angle approximation the EWA provides no information on the experimentally important transverse momentum spectrum of the final state jets or of the diboson in the $qq \rightarrow qqWW$ process used to observe WW scattering at hadron colliders. In addition to reviewing the EWA I will also describe the effective Higgs boson method[11], which provides complete information on the final state particles and also retains interference of signal and background amplitudes that is neglected by the EWA.

5.1 Effective W approximation

The effective W approximation is analogous to the effective photon approximation of Weiszacker and Williams. It provides an effective luminosity distribution for the probability to find colliding “beams” of longitudinally polarized gauge bosons within the colliding quark “beams” produced at a pp collider or within the l^+l^- beams at a lepton collider. For incident fermions f_1 and f_2 the effective luminosity for longitudinally polarized gauge bosons V_1 and V_2 is

$$\left. \frac{\partial \mathcal{L}}{\partial z} \right|_{V_1 V_2 / f_1 f_2} = \frac{\alpha^2 \chi_1 \chi_2}{\pi^2 \sin^4 \theta_W} \frac{1}{z} \left[(1+z) \ln \left(\frac{1}{z} \right) - 2 + 2z \right] \quad (5.1)$$

where $z \equiv s_{VV}/s_{ff}$ and the χ_i are the $f_i - V_i$ couplings, e.g., $\chi_W = 1/4$ for all fermions, $\chi_{Zu\bar{u}} = (1 + (1 - \frac{8}{3} \sin^2 \theta_W)^2)/16 \cos^2 \theta_W$, etc ... Equation (5.1) must be convoluted with the desired $V_1 V_2$ subprocess cross section and also with the quark distribution functions in the case of pp collisions,

$$\sigma(pp \rightarrow \dots) = \int_{\tau} \left. \frac{\partial \mathcal{L}}{\partial \tau} \right|_{qq/pp} \cdot \int_x \sum_{V_L} \left. \frac{\partial \mathcal{L}}{\partial x} \right|_{V_L V_L / qq} \cdot \sigma(V_L V_L \rightarrow \dots) \quad (5.2)$$

The effective W approximation has been compared with analytical and numerical evaluations of Higgs boson production. The analytical calculations[29] show good agreement for $WW \rightarrow H$ for $m_H \geq 500$ GeV, with errors $\lesssim O(10\%)$ and decreasing with m_H and \sqrt{s} , while for the relatively less important process $ZZ \rightarrow H$ the errors are roughly twice as large. Above 1 TeV the errors are very small.

5.2 Effective Higgs boson

Because it is a small angle approximation the EWA tells us nothing about the transverse momentum of the final state quark jets. As discussed in section 6, a central jet veto and/or forward jet tag are useful experimental strategies, requiring knowledge of both signal and background jet p_T distributions. Common practice is to use the EWA while assuming that the jet p_T distribution for strong WW scattering is the same as that of the standard model with a 1 TeV Higgs boson. Near the edge of phase space, as we are in the study of the WW

system at ≥ 1 TeV at the LHC, the the jet p_T distribution varies with the WW invariant mass. The EHB method[11] provides the appropriate final state p_T distribution for any s-wave strong scattering model. In addition, because the collider signal is computed from the model *amplitude*, not the cross section as in eq. 5.2, the EHB retains phase information and signal-background interference effects that are lost in the EWA.

Consider a strong s-wave scattering model ‘ X ’, formulated in an R-gauge as a Goldstone boson scattering amplitude, for instance, the leading $J = 0$ component of $\mathcal{M}^X(w^+w^- \rightarrow zz)$. To leading order in the $SU(2)_L$ coupling constant g we decompose the corresponding $W_L^+W_L^- \rightarrow Z_LZ_L$ amplitude into gauge sector and symmetry-breaking sector contributions,

$$\mathcal{M}_{\text{Total}}^X(W_LW_L) = \mathcal{M}_{\text{Gauge}}(W_LW_L) + \mathcal{M}_{\text{SB}}^X(W_LW_L). \quad (5.3)$$

$\mathcal{M}_{\text{Gauge}}$ is the sum of W , γ , and Z exchange diagrams; it increases like E^2 for large E ,

$$\mathcal{M}_{\text{Gauge}} = g^2 \frac{E^2}{M_W^2} + \mathcal{O}(g^2, E^0). \quad (5.4)$$

This order E^2 term is precisely the “bad high energy behavior” discussed in section 2 that $\mathcal{M}_{\text{SB}}^X(W_LW_L)$ must cancel. It is also precisely the low energy theorem amplitude, as can be seen by comparing eq. 5.4 with eqs. 2.34 and 2.36. This is no coincidence[13]: if the symmetry breaking force is strong, the quanta of the symmetry breaking sector are heavy, $M_{\text{SB}} \gg M_W$, and decouple in gauge boson scattering at low energy, $\mathcal{M}_{\text{SB}}^X \ll \mathcal{M}_{\text{Gauge}}$. Then the quadratic term in $\mathcal{M}_{\text{Gauge}}$ dominates $\mathcal{M}_{\text{Total}}$ for $M_W^2 \ll E^2 \ll M_{\text{SB}}^2$, which establishes the low energy theorem to order g^2 without using the ET. Thus we may also write

$$\mathcal{M}_{\text{LET}} = \frac{s}{v^2} = \mathcal{M}_{\text{Gauge}} + \mathcal{O}(g^2, E^0). \quad (5.5)$$

We next use the equivalence theorem to assert the approximate equality of the U-gauge amplitude with the model amplitude formulated in R-gauge,

$$\mathcal{M}_{\text{Total}}^X(W_LW_L) = \mathcal{M}_{\text{Goldstone}}^X(ww) + \mathcal{O}(g^2, E^0). \quad (5.6)$$

Combining eqs. 5.4 - 5.6 we find the corresponding contribution of the symmetry breaking sector to the U-gauge W_LW_L amplitude,

$$\mathcal{M}_{\text{SB}}^X(W_LW_L) = \mathcal{M}_{\text{Goldstone}}^X(ww) - \mathcal{M}_{\text{LET}} + \mathcal{O}(g^2, \frac{M_W}{E}). \quad (5.7)$$

Finally we reexpress eq 5.7 in terms of an effective Higgs boson propagator, P_{EFF}^X , constructed to be exchanged in the s-channel with standard model WW and ZZ couplings,

$$P_{\text{EFF}}^X(s) = -i \frac{v^2}{s^2} (\mathcal{M}_{\text{Goldstone}}^X(ww) - \mathcal{M}_{\text{LET}}), \quad (5.8)$$

defined so that its s-channel exchange reproduces equation (5.7). Notice that \mathcal{M}_{LET} contributes i/s to P_{EFF}^X , corresponding to a massless scalar pole, making explicit the connection between the spontaneously broken symmetry that implies \mathcal{M}_{LET} and the cancellation of the

bad high energy behavior by Higgs boson exchange. The residual contribution to P_{EFF}^X from $\mathcal{M}_{\text{Goldstone}}^X$ carries the model dependent strong interaction dynamics.

We can use $P_{\text{EFF}}^X(s)$ in any gauge to extract the consequences of model X . To compute the predicted collider signal, we compute the full standard model set of Feynman diagrams for $qq \rightarrow qqWW/ZZ$ using $P_{\text{EFF}}^X(s)$ for the Higgs boson propagator. It is shown in references [11] that the method agrees with the EWA where it should, while improving on the EWA at small angles where it includes interference with the photon t-channel exchange amplitude that is neglected in the EWA. Just as in the tree-level evaluation of SM Higgs boson production, it provides a complete description of the final state. It is also shown, in the second of references[11], that the amplitudes are BRS invariant.

6. Can LHC lose?

This section offers a sketch of strong WW scattering at the LHC, with the strategies to enhance the signals relative to the backgrounds and an estimate of the integrated luminosity needed to either confirm or exclude the signals. The discussion will focus on the chiral “ ρ ” effective Lagrangian. As described in section 4 it illustrates the complementary interplay between resonant and nonresonant signals, and in the $m_\rho \rightarrow \infty$ limit approaches the nonresonant K-matrix model. We consider WZ scattering which the “ ρ ” resonance would enhance and like-charge W^+W^+ scattering which chiral invariant “ ρ ” exchange would suppress. Discussion of other models and channels may be found in references [6, 30].

6.1 W^+W^+ elastic scattering

The W^+W^+ and W^-W^- channels are interesting for three reasons:

- They do not have the $\bar{q}q \rightarrow WW$ or $gg \rightarrow WW$ backgrounds, respectively of order α_W and $\alpha_W\alpha_S$ in amplitude, that are the dominant backgrounds to strong scattering in other gauge boson pair channels.
- The branching ratio for $W^+W^+ \rightarrow l^+\nu + l^+\nu$ with $l = e$ or μ is relatively large, $\sim 5\%$, and has a striking experimental signature: two isolated, high p_T , like-sign leptons in an event with no other significant activity (jet or leptonic) in the central region.
- Strong $W^+W^+ + W^-W^-$ scattering complements the strong scattering signals in the other gauge boson pair channels, and is likely to be largest if the resonance signals expected in the other channels are smallest.

The W^+W^+ strong scattering signal was first estimated in ref.[1] but with no estimate of the backgrounds. There have subsequently been several more detailed studies of signals and backgrounds,[31] resulting in a powerful set of cuts. One would expect the $O(\alpha_S\alpha_W)$ gluon exchange amplitude for $qq \rightarrow qqW^+W^+$ to be the dominant background, but, surprisingly, after cuts it is much smaller than the electroweak $O(\alpha_W^2)$ background.[32] Even more surprising, $\bar{q}q \rightarrow W^+Z$ [33, 5] and $\bar{q}q \rightarrow W^+\gamma^*$ [5] with the negative charge lepton escaping detection are as important as the irreducible $qq \rightarrow qqW^+W^+$ backgrounds. (Backgrounds from W^+W^- production with mismeasurement of a lepton charge and top quark related backgrounds[26, 34] can be controlled and are not considered here.)

While a forward jet tag may provide further background suppression, the results quoted below, from [5], rely only on hard lepton cuts and a central jet veto (CJV) of events containing

a jet with central rapidity, $\eta_J < 2.5$ and high transverse momentum, $P_T(J) > 60$ GeV. The CJV reduces backgrounds from transversely polarized W bosons, which are emitted at larger transverse momenta than the longitudinally polarized W bosons of the signal. The hard lepton cuts rely on the general property that the strong scattering subprocess cross sections increase with s_{WW} while the backgrounds scale like $1/s_{WW}$, and on the differing polarization of the signal and background WW pairs. If this strategy suffices it has the advantage of being cleaner than relying on forward jet tagging, which may be subject to QCD corrections and to detector-specific jet algorithms and acceptances in the forward region.

The leptonic cuts are optimized for each set of model parameters. It turns out for the four values of m_ρ considered that the rapidity and lepton transverse momentum cuts are $\eta(l) < 1.5$ and $p_T(l) > 130$ GeV. A third cut, requiring the two leptons to be back-to-back in azimuth, depends somewhat on m_ρ .

The WZ and $W\gamma^*$ backgrounds — actually the complete background from all amplitudes for $\bar{q}q \rightarrow l^+\nu l^-$ — in which the l^- escapes detection, occurs because any detector has unavoidable blind spots at low transverse momentum and at high rapidity. At very low p_T , muons will not penetrate the muon detector, electrons or muons may be lost in minimum bias pile-up, and for low enough p_T in a solenoidal detector they will curl up unobservably within the beam pipe. Muon and electron coverage is also not likely to extend to the extreme forward, high rapidity region.

In reference [5] an attempt was made to employ reasonable though aggressive assumptions about the observability of the extra electron or muon. Rapidity coverage for electrons and muons was assumed for $\eta(l) < 3$. Within this rapidity range it was assumed that isolated e^- and μ^- leptons with $p_T(l) > 5$ GeV can be identified in events containing two isolated, central, high p_T e^+ 's and/or μ^+ 's. It was also assumed that electrons (but not muons) with $1 < p_T(l) < 5$ GeV can be identified if they are sufficiently collinear ($m(e^+e^-) < 1$ GeV) with a hard positron in the central region. For $p_T(e^-) < 1$ GeV electrons were considered to be unobservable.

A robust observability criterion is defined and the cuts are optimized by searching over the cut parameter space for the set of cuts that satisfy the observability criterion with the smallest integrated luminosity. The criterion is

$$\sigma^\dagger = S/\sqrt{B} \geq 5 \quad (6.1)$$

$$\sigma^\ddagger = S/\sqrt{S+B} \geq 3 \quad (6.2)$$

$$S \geq B, \quad (6.3)$$

where S and B are the number of signal and background events, and σ^\dagger and σ^\ddagger are respectively the number of standard deviations for the background to fluctuate up to give a false signal or for the signal plus background to fluctuate down to the level of the background alone. The σ^\ddagger criterion is essential to assure the ability to exclude strong scattering if it does not exist. In addition $S \geq B$ is required so that the signal is unambiguous despite the systematic uncertainty in the size of the backgrounds, which will probably be known to better than $\leq \pm 30\%$ after ‘‘calibration’’ studies with known processes at the LHC. An experiment meeting this criterion, eqs. 6.1 - 6.3, can definitively establish the existence

Table 6.1 Minimum integrated luminosity \mathcal{L}_{MIN} to satisfy significance criterion for $W^+W^+ + W^-W^-$ scattering. Also shown are the optimum cuts, the corresponding number of signal and background events per 100 fb^{-1} , and the composition of the background for the optimum cut. Rejection of all events for which the third (wrong-sign) lepton falls within its acceptance region is assumed.

$m_\rho(\text{TeV})$	1.78	2.06	2.52	4.0
$\mathcal{L}_{MIN} (\text{fb}^{-1})$	142	123	105	77
<i>WW Cut</i>				
$\eta^{MAX}(l)$	1.5	1.5	1.5	2.0
$p_T^{MIN}(l) (\text{GeV})$	130.	130.	130.	130.
$[\cos \phi(l)]^{MAX}$	-0.72	-0.80	-0.80	-0.90
<i>WW Sig/Bkgd</i>				
(events per 100 fb^{-1})	12.7/6.0	14.1/5.8	15.9/5.8	22.4/8.9
<i>WW Backgrounds (%)</i>				
$\bar{l}l\nu_l$	47	49	49	61
$O(\alpha_W^2)$	47	46	46	33
$O(\alpha_W\alpha_S)$	6	6	6	6

of strong scattering if it exists or exclude it if it does not. As discussed in the introduction, the latter capability is as important as the former. The criteria are applied to the actual event yields after correcting for detector efficiency, assumed to be 85% for each isolated lepton falling within the region defined by the cuts.

The results are collected in table 6.1 for four values of the “ ρ ” mass. We see that the heaviest value of m_ρ gives the largest signal, requiring the smallest integrated luminosity, $\mathcal{L}_{MIN} = 77 \text{ fb}^{-1}$, less than a year of running at the design luminosity of $10^{34} \text{ cm}^{-2}\text{sec}^{-1}$. The nonresonant K-matrix and linear models provide similar though slightly bigger signals. For the lightest mass considered, about $1\frac{1}{2}$ years would be needed. In tables 6.1 - 6.3 the event yields per 100 fb^{-1} do not include detector efficiency while \mathcal{L}_{MIN} does.

Table 6.1 assumes 100% veto efficiency when the third lepton in the $l^+\nu l^-$ background falls within the geometric acceptance specified above. Table 6.2 shows the effect of veto inefficiency for $m_\rho = 2.52 \text{ TeV}$. At 98% efficiency the effect is not great but at 95% $\mathcal{L}_{MIN}(WZ)$ is increased by 40%. For 90%, not shown in the table, $\mathcal{L}_{MIN}(WZ)$ would be nearly doubled, to 200 fb^{-1} . Hopefully an aggressive $\simeq 98\%$ efficient veto is possible without significantly affecting the signal efficiency. The question clearly depends on the capability of the particular detectors.

6.2 The WZ signal

The WZ signal arises from two separate mechanisms.[1] The first is elastic WZ scattering via $qq \rightarrow qqWZ$ where the $WZ \rightarrow WZ$ subprocess is mediated by s-channel and u-channel ρ exchange as well as the contact interactions required by chiral symmetry.[4] The second is by $\bar{q}q \rightarrow \rho$, evaluated using ρ dominance. The backgrounds are $\bar{q}q \rightarrow WZ$ and $qq \rightarrow qqWZ$, the latter from both the $O(\alpha_W^2)$ and $O(\alpha_W\alpha_S)$ amplitudes. The $O(\alpha_W^2)$ background amplitude is the $qq \rightarrow qqWZ$ cross section from $SU(2) \times U(1)$ gauge interactions, computed in the standard model with a light Higgs boson, say $m_H \leq 0.1 \text{ TeV}$.

Table 6.2 Minimum luminosity to satisfy significance criterion for $W^+W^+ + W^-W^-$ scattering for $m_\rho = 2.52$ TeV, assuming 100%, 98% or 95% efficiency for the veto of wrong-sign charged leptons that fall within the acceptance region specified in the text. The optimum cuts and corresponding yields are shown as in table 1.

Efficiency	100%	98%	95%
$\mathcal{L}_{MIN}(WW)$ (fb^{-1})	105	115	148
<i>WW Cut</i>			
$\eta^{MAX}(l)$	1.5	1.5	1.5
$p_T^{MIN}(l)$ (GeV)	130.	130.	160.
$[\cos \phi(l)]^{MAX}$	-0.80	-0.80	-0.86
<i>WW Sig/Bkgd</i>			
(events/100 fb^{-1})	15.9/5.8	15.9/7.9	12.1/5.6
<i>WW Backgrounds (%)</i>			
$\bar{l}l\nu_l$	49	62	71
$O(\alpha_W^2)$	46	34	26
$O(\alpha_W\alpha_S)$	6	4	3

The results presented here are taken from reference [4]. The signal is observed in the decay channel $WZ \rightarrow l\nu + \bar{l}l$ where $l = e$ or μ , with net branching ratio $BR = 0.0143$. A central jet veto is applied as in section 6.1. Because the signals occur at enormous WZ energy they stand out prominently and simple cuts suffice — on the lepton rapidity $\eta_l < \eta_l^{MAX}$, the azimuthal angles ϕ_{ll} between the leptons from the Z and the charged lepton from the W , $\cos\phi_{ll} < (\cos\phi_{ll})^{MAX}$, and the Z transverse momentum, $p_{TZ} > p_{TZ}^{MIN}$. The cuts are optimized for each choice of m_ρ to minimize the integrated luminosity satisfying eqs. 6.1 - 6.3. The detector efficiency for $WZ \rightarrow l\nu + \bar{l}l$ is estimated[35] to be $0.85 \times 0.95 \simeq 0.8$.

The results are summarized in table 6.3, for three values of m_ρ . The signal for $m_\rho = 1.78$ TeV is easily visible, meeting the observability criterion with less than a half year at design

Table 6.3 Minimum luminosity to satisfy observability criterion for $W^\pm Z$ scattering for $m_\rho = 1.78, 2.52, 4.0$ TeV. Each entry displays \mathcal{L}_{MIN} in fb^{-1} , the number of signal/background events per 100 fb^{-1} , and the corresponding values of the cut parameters $\eta^{MAX}(l)$, p_{TZ}^{MIN} , and $\cos(\phi_{ll})^{MAX}$. A central jet veto is applied as discussed in the text.

m_ρ (TeV)	1.78 TeV	2.52 TeV	4.0 TeV
$\mathcal{L}_{MIN}(WZ)$ (fb^{-1})	44 fb^{-1}	300 fb^{-1}	no signal
<i>Cuts</i>			
$\eta^{MAX}(l)$	2	2	
$p_{TZ}^{MIN}(l)$ (GeV)	450	675	
$[\cos \phi(l)]^{MAX}$	1.0	1.0	
<i>$W^\pm Z$ Sig/Bkgd</i>			
(events/100 fb^{-1})	38/20	5.8/3.4	

luminosity. (The signal for $m_\rho = 2.06$ TeV [corresponding to $SU(3)_{TC}$] is not shown in the table; it requires 98fb^{-1} to meet the criterion.) The heaviest mass considered, $m_\rho = 4$ TeV, is indistinguishable at the LHC from nonresonant scattering models; it provides no signal consistent with eq. 6.3. The $m_\rho = 2.52$ TeV signal ($SU(2)_{TC}$) requires three years at design luminosity.

6.3 The bottom line

Comparing tables 6.1 and 6.3 the complementarity of the nonresonant W^+W^+ channel and the resonant WZ channel is clear. The lightest value of m_ρ provides the smallest W^+W^+ signal and the largest, readily observable WZ signal. Models with very heavy m_ρ or of nonresonant strong scattering cannot be observed in the WZ channel for any luminosity while satisfying eq. 6.3, but they provide the largest signals in W^+W^+ scattering.

The over-all worst case, intermediate between these extremes, is the value of m_ρ for which $\text{MIN}(\mathcal{L}_{\text{MIN}}(WZ), \mathcal{L}_{\text{MIN}}(W^+W^+))$ is largest. This turns out to be $m_\rho = 2.52$ TeV, corresponding to $SU(2)_{TC}$, for which the best signal is in the W^+W^+ channel. It determines the “no-lose” luminosity needed to observe strong scattering in at least one channel. As shown in table 6.2, this luminosity depends on the experimental veto efficiency for wrong-sign leptons that fall within the experimental acceptance. Following the slogan “when in doubt throw it out,” it may be possible to achieve 98% veto efficiency without significantly eroding the efficiency for the signal, in which case little more than one year at design luminosity would suffice. More pessimistically, with 95% veto efficiency, one and a half years would be needed.

7. Conclusion

Only direct discovery and detailed study of the symmetry breaking quanta can establish the nature of the symmetry breaking sector in a model-independent way. The ability to measure strong WW scattering is an important part of the experimental program whether electroweak symmetry breaking is strong or not. Given this capability we can determine the mass scale of the symmetry breaking sector even if its constituent quanta initially escape detection at the LHC. And even if a light Higgs boson is discovered, we would want to verify the absence of strong WW scattering, a fundamental prediction of theories in which symmetry breaking is dominated by light Higgs bosons.

The strong WW scattering signals are challenging: they push the LHC to the limits of its reach. The theoretical estimates of the possibility of detecting strong WW scattering at the LHC may seem simple and optimistic. But, as we have learned from the Higgs boson searches at LEP, experimenters working with real detectors and real data can invent and validate clever strategies that exceed even the most optimistic of the early theoretical simulations.

Can LHC lose? — No, not likely, as long as the accelerator and detectors succeed in reaching the ambitious design goals.

Acknowledgements: I wish to thank Dirk Graudenz, Milan Locher, and Christine Kunz for a very stimulating and pleasant week. This work was supported by the Director, Office of Energy Research, Office of High Energy and Nuclear Physics, Division of High Energy Physics of the U.S. Department of Energy under Contract DE-AC03-76SF00098.

References

- [1] M.S. Chanowitz and M.K. Gaillard, *Nucl. Phys.* B261, 379 (1985).
- [2] B. Holdom, *Phys.Rev.* D54:721(1996), hep-ph/9602248; R. Casalbuoni et al., *Phys.Rev.* D56:5731(1997), hep-ph/9704229; B. Dobrescu and J. Terning, *Phys.Lett.* B416:129(1998), hep-ph/9709297; B. Dobrescu and E. Simmons, hep-ph/9807469; B. Holdom and T. Torma, hep-ph/9807561.
- [3] J. Gunion, H. Haber and T. Moroi, hep-ph/9610337.
- [4] M. Chanowitz and W. Kilgore, *Phys.Lett.*B322:147(1994), hep-ph/9311336.
- [5] M. Chanowitz and W. Kilgore, *Phys.Lett.*B347:387(1995), hep-ph/9412275.
- [6] J. Bagger et al., *Phys.Rev.*D52:3878(1995), hep-ph/9504426.
- [7] J. Espinosa, J. Gunion, hep-ph/9807275.
- [8] J.M. Cornwall, D.N. Levin, and G. Tiktopoulos, *Phys. Rev.* D10, 1145 (1974); C.E. Vayonakis, *Lett. Nuovo Cim.* 17, 383 (1976); B.W. Lee, C. Quigg, and H. Thacker, *Phys. Rev.* D16, 1519 (1977).
- [9] M.S. Chanowitz and M.K. Gaillard, ref.1; G. Gounaris, R. Kögerler, and H. Neufeld, *Phys. Rev.* D34, 3257(1986); H. Veltman, *Phys. Rev.* D41, 2294(1990); J. Bagger and C. Schmidt, *Phys. Rev.* D41, 264 (1990); W. Kilgore, *Phys. Lett.* 294B, 257(1992); H-J. He, Y-P. Kuang, X-Y. Li, *Phys. Rev. Lett.* 69, 2619 (1992) and *Phys. Rev.* D49, 4842 (1994); H-J. He and W. Kilgore, *Phys.Rev.*D55:1515(1997), hep-ph/9609326.
- [10] M.S. Chanowitz and M.K. Gaillard, *Phys. Lett.* 142B, 85 (1984) and ref. 1; G. Kane, W. Repko, B. Rolnick, *Phys. Lett.* B148, 367 (1984); S. Dawson, *Nucl. Phys.* B29, 42 (1985).
- [11] M. Chanowitz, *Phys.Lett.*B373:141(1996), hep-ph/9512358; *Phys.Lett.*B388:161(1996), hep-ph/9608324.
- [12] M. Weinstein, *Phys. Rev.* D8, 2511(1973); S. Weinberg, *Phys. Rev.* D13, 974(1976) and D19, 1277(1979); L. Susskind, *Phys. Rev.* D20, 2619(1979).
- [13] M.S. Chanowitz, M. Golden, and H.M. Georgi, *Phys. Rev.* D36, 1490(1987); *Phys. Rev. Lett.* 57 2344(1986).
- [14] S. Weinberg, *Phys. Rev. Lett.* 17, 616(1966).
- [15] T.D. Lee and C.N. Yang, *Phys. Rev. Lett.* 4, 307(1960).
- [16] B.L. Ioffe, L.B. Okun, and A.P. Rudik, *Sov. Phys. JETP Lett.* 20, 128(1965).
- [17] M.K. Gaillard, *Phys. Lett.*B 293, 410(1992).

- [18] S. Dittmaier, D. Schildknecht, and G. Weiglein, *Phys. Lett.* B386, 247,1996.
- [19] A. Gurtu, *Phys. Lett.* B385, 415, 1996.
- [20] G. Degrassi, P. Gambino, M. Passera, A. Sirlin, *Phys.Lett.*B418:209(1998), e-print hep-ph/9708311, and references therein.
- [21] M. Chanowitz, *Phys. Rev. Lett.* 80:2521(1998), e-print hep-ph/9710308; and LBL-42103, hep-ph/9807452, submitted to *Phys. Rev.D*.
- [22] Particle Data Group, R.M. Barnett *et al.*, *Eur. Phys. J.*C3,1(1998).
- [23] D. Karlen, presented at the 29'th Intl. Conf. on HEP, Vancouver, July 23-29, 1998, to be published in the proceedings; M. Grünwald, *ibid*.
- [24] T. Barklow *et al.*, Proc. DPF / DPB Summer Study on New Directions for High-Energy Physics (Snowmass 96), hep-ph/9704217; W. Kilgore, *ibid*, hep-ph/9610375.
- [25] M. Chanowitz, in *Perspectives on Higgs Physics II*, ed. G. Kane, World Scientific, Singapore, 1997.
- [26] V. Barger, K. Cheung, T. Han, and R. Phillips, *Phys. Rev. D*42 3052 (1990).
- [27] S. Weinberg, *Phys. Rev.* 166, 1568(1968).
- [28] R. Casalbuoni *et al.*, *Phys. Lett.* 155B, 95 (1985); *Nucl. Phys.* B282, 235 (1987).
- [29] G. Altarelli, B. Mele, and F. Pitolli, *Nucl. Phys.* B287, 205 (1987).
- [30] M. Berger and M. Chanowitz, *Phys.Rev.Lett.*68, 757(1992).
- [31] V. Barger, K. Cheung, T. Han, and R. Phillips, *Phys. Rev. D*42. 3052 (1990); D. Dicus, J. Gunion, and R. Vega, *Phys. Lett.* 258B, 475(1991); D. Dicus, J. Gunion, L. Orr, and R. Vega, *Nucl.Phys.*B377, 31(1992); M. Berger and M.S. Chanowitz, *Phys. Lett.* 263B, 509(1991) .
- [32] D. Dicus and R. Vega, *Nucl. Phys.* B329, 533 (1990).
- [33] G. Azuelos, C. Leroy, and R. Tafirout, ATLAS Internal Note PHYS-NO-033, 1993 (unpublished); G. Azuelos, talk presented at CERN, April 21, 1994 (unpublished).
- [34] D. Dicus *et al.*, reference [31].
- [35] Solenoidal Detector Collaboration, E.L. Berger *et al.*, *Technical Design Report*, SDC-92-201, 1992.

**ERNEST ORLANDO LAWRENCE BERKELEY NATIONAL LABORATORY
ONE CYCLOTRON ROAD | BERKELEY, CALIFORNIA 94720**